XV International Conference on Durability of Building Materials and Components
DBMC 2020, Barcelona
C. Serrat, J.R. Casas and V. Gibert (Eds)

A Spatially Continuous Driving Rain Map of India at 0.5°×0.5° Gridded Scale

Sneha Das[1] **and Kaustav Sarkar**[2]

[1]School of Engineering, Indian Institute of Technology Mandi, Kamand, Himachal Pradesh-175075, India, D16031@students.iitmandi.ac.in

[2]School of Engineering, Indian Institute of Technology Mandi, Kamand, Himachal Pradesh-175075, India, srkr@iitmandi.ac.in

Abstract. *Driving rain is one of the most critical sources of moisture affecting the hygrothermal and durability performance of building envelopes. The estimation of severity in terms of annual driving rain indices using annual and monthly weather data (aaDRI and maDRI respectively) aids towards contemplating potential moisture loads, and hence in the efficient design of buildings in the geographical area of interest. In this study, monthly and annual gridded datasets of wind and rainfall, pertaining to the thirty-year period of 1988-2017 have been used to design a spatially continuous driving rain map for India at 0.5°×0.5° (lat./long.) resolution. The observations reveal that the use of annually averaged data leads to underestimation of the driving rain severity thereby highlighting the inefficiency of a coarser temporal scale. A linear relationship has subsequently been developed to enable refinement of aaDRI into maDRI. The analysis of the monthly driving rain map reveals that the entire western coastal belt and a few regions in the north-eastern part of the country observe high to severe exposure conditions. Furthermore, a trend analysis of the yearly driving rain index values reveals statistically significant decreasing trends over the northern and eastern regions of the country, whereas increasing trends in the shielded regions surrounding central India is observed.*

Keywords: *Driving Rain Map, Gridded Data, Trend Analysis, India.*

1 Introduction

Durability performance of built facilities is a function of both the material characteristics and the environment to which they are exposed. The exposure conditions that primarily affect the durability include temperature and moisture conditions. The presence of moisture initiates and escalates numerous deterioration processes in building materials. Damage is often inflicted in the form of cracks and/or spalling of surface due to corrosion of reinforcement, and salt migration and crystallization (Broomfield, 2003; Charola, 2000; Neville, 1995). Prolonged dampness also leads to efflorescence and mold growth, which affects the aesthetics as well as the indoor air quality of buildings (Gaylarde *et al*., 2002; Bornehag *et al.*, 2001). Moisture accumulation in porous materials causes frost damage and a reduction in thermal insulation of the building envelope (Bhattacharjee, 2013; Jerman and Černý, 2012). The intricate and multifaceted impact of moisture on the performance of buildings invokes the need to realistically estimate the severity of moisture exposure.

Wind Driven Rain (WDR) is an important source of moisture affecting the hygrothermal performance and durability of building facades (Blocken *et al*., 2009). A significant development in the field of WDR research was associated with the field observations made

by Lacy (1965) and Hoppestad (1955), which established the proportionality of WDR intensity (R_{wdr}), to horizontal rainfall (R_h), and the wind speed (U). This proportionality relationship led to the development of WDR index $(R_h * U)$, and its application to map the driving rain severity in several countries (Narula *et al.*, 2017; Pérez-Bella *et al.*, 2012; Giarma, 2011; Chand and Bhargava, 2002). A schematic representation of WDR is depicted in Fig. 1.

The accuracy and reliability of such maps depend upon the spatial and temporal resolution of available meteorological data. The station records available in a country are often limited and lack temporal completeness. Gridded weather data poses a viable solution in this regard owing to their temporal and spatial consistency (Das *et al*., 2020). This study utilizes monthly average wind and rainfall gridded data to determine the *maDRI* and *aaDRI* at a spatial resolution of $0.5° \times 0.5°$ for the Indian subcontinent.

To the best of the authors' knowledge, the WDR map generated in this study offers the finest spatial resolution at which the *maDRI* and *aaDRI* have been mapped for Indian mainland. The numerical efficiency of the gridded data and the developed index is also verified by comparing the relationship between *maDRI* and *aaDRI* against previously reported studies by Chand and Bhargava (2002) and Narula *et al*. (2017). The results of this study are in close conformance with the previous studies. The study also extends to the trend analysis of driving rain index for the recent 30 years of weather records (1988-2017). Trend analysis of the WDR over India shows a receding trend of moisture loads over the country.

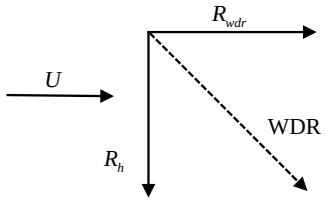

Figure 1. Components of wind-driven rain (WDR).

2 Gridded Data

Gridded datasets are interpolated products constituted using observations from sources like station observations, satellites, ships etc. and have the benefit of temporal continuity and spatial coverage. The present study uses gridded datasets of rainfall and wind for the determination of driving rain severity. The study uses thirty years of rainfall and wind data from 1988-2017.

2.1 Rainfall Data

Rainfall gridded dataset at a monthly scale has been obtained from the Climatic Research Unit (CRU) - version CRU TS v4.02. The data is based on station observations collected from reliable international agencies and covers all land masses excluding the Antarctica region at $0.5° \times 0.5°$ (lat./long.) resolution. The stations selected for the generation of data at individual grids is subjected to the criteria of minimum 75% data availability for the base period, 1961-1990 (Harris *et al.*, 2014). Out of the global dataset, rainfall data for 1179 grids pertaining to

the duration 1988-2017 have been extracted, which encompasses the geographical stretch of India lying within a rectangular region extending between 6.5°N - 37.5°N to 66.5°E - 101.5°E.

2.2 Wind Data

Monthly wind data have been obtained from the web repositories of the National Oceanic and Atmospheric Administration (NOAA). The dataset is available at a spatial resolution of $2.5° \times 2.5°$ between 90°N - 90°S and 0°E - 357.5°E (NOAA, 2019). Both horizontal and vertical components of wind records for India which comprises of 1179 grid values, have been extracted from the primary global dataset. The extracted records for the Indian region have been re-gridded to a resolution of $0.5° \times 0.5°$ for the purpose of this study using bilinear interpolation. The resultant wind vector was determined as: $\left(u^2 + v^2\right)^{0.5}$ where *u* and *v* are the horizontal and vertical wind components respectively.

3 Driving Rain Index

3.1 Calculation of *maDRI* and *aaDRI*

The procedure for determination of *maDRI* and *aaDRI* is adopted from previous studies (Chand and Bhargava, 2002; Giarma and Aravantinos, 2011). Firstly, the monthly driving rain index (*mDRI*) for each of the 12 months have been calculated using Eq. 1 and then the *maDRI* has been calculated using Eq. 2.

$$mDRI = \left(\sum_{i=1}^{N} W_{month,i} / N\right)\left(\sum_{i=1}^{N} R_{month,i} / N\right) \tag{1}$$

$$maDRI = \sum_{i=1}^{12} mDRI \tag{2}$$

where, *maDRI* is in m^2/s, W_{month} is the monthly average wind speed in *m/s*, R_{month} is the monthly total rainfall in *m*, *N* is the number of years under consideration. The estimation of *mDRI* can be carried out by including the cases for which rainfall is zero, or by excluding such instances for averaging of the rainfall. The latter approach is expected to provide a more realistic depiction. In this study, the *mDRI* values have been determined by both approaches to assess the differences in results obtained by the two approaches.

The *aaDRI* has been calculated as the product of average annual wind speed and average annual rainfall, as stated in Eq. 3.

$$aaDRI = \left(\sum_{i=1}^{N} W_{year,i} / N\right)\left(\sum_{i=1}^{N} R_{year,i} / N\right) \tag{3}$$

where *aaDRI* is in m^2/s, W_{year} is the annual average wind speed in *m/s*, R_{year} is the annual total rainfall in *m*, *N* is the number of years under consideration.

Based on the values of indices calculated using Eqs. 2 and 3, the exposure conditions have been categorized into four classes after Lacy (1977), namely, shielded, moderate, high, and severe for the ranges of [0,3), [3,7), [7,11), and [11, ∞), respectively. This classification has been subsequently used towards the development of *maDRI* and *aaDRI* maps for India.

Often meteorological data are not available at a monthly temporal scale. This study, therefore, establishes a relationship between *aaDRI* and *maDRI* to facilitate estimation of the latter from annual meteorological records which are often available.

3.2 Trend Analysis

A trend analysis of the yearly driving rain index (*yDRI*) has been carried out to ascertain the increasing or decreasing pattern of driving rain severity across the subcontinent. Mann-Kendall (MK) test is a non-parametric test commonly used to statistically assess any monotonic upward or downward trend in a time series data (Mann, 1945). The present study uses this test to identify the existence of trends in the manifestation of driving rain over the Indian mainland. In this test, the null hypothesis is that data comes from a sample of independent realizations, and hence there is no trend in the data, whereas the alternative hypothesis states that a monotonic trend exists. The MK test statistic is calculated using Eqs. 4 and 5:

$$S = \sum_{k=1}^{n-1} \sum_{j=k+1}^{n} \operatorname{sgn}\left(X_j - X_k\right) \tag{4}$$

such that,

$$\operatorname{sgn}(X_j - X_k) = \begin{cases} 1, \ if \ (X_j - X_k) > 0 \\ 0, \ if \ (X_j - X_k) = 0 \\ -1, \ if \ (X_j - X_k) < 0 \end{cases} \tag{5}$$

Here, $j \neq k$, and $j, k \leq n$, where n is the number of data points. The *z*-statistic is then computed as stated in Eq. 6:

$$Z_s = \begin{cases} \dfrac{S-1}{\sqrt{Var(S)}}, S > 0 \\ 0, \quad S = 0 \\ \dfrac{S+1}{\sqrt{Var(S)}}, S < 0 \end{cases} \tag{6}$$

If $|Z_s| > Z_{1-\alpha/2}$ ($Z_{1-\alpha/2}$ can be obtained from standard normal distribution level), then the null hypothesis is rejected. In the present study, the test is carried out at $\alpha = 0.05$ significance level. The trend analysis is also supported by the determination of Sen's slope. The Sens's slope (β) assists in the determination of direction of the existing trend. In the case of driving rain, the Sen's slope estimates if the driving rain severity is decreasing or increasing. This helps a designer to contemplate if a building will be exposed to a greater moisture load and thereby help towards efficient design of facade elements.

4 Results and Discussions

4.1 Driving Rain of India Based on *maDRI* and *aaDRI*

Figs. 2a and 2b represent the *maDRI* maps obtained respectively by including and excluding the cases for which rainfall is zero. It was observed that there is no significant difference between the *maDRI* maps developed using the two approaches. The plots reveal that the

shielded exposure region covers major area of northern part of the country, along with parts of central, western, and south-western India. The moderate exposure covers the entire eastern coastal belt and majority of north-eastern India, in addition to parts of western and central India. The high and severe exposure condition, is observed by the western coastal belt of India and parts of north-east. This observation is common for both the approaches adopted in the determination of *maDRI*. The percentage of land area covered by each of the exposure categories using the latter approach are 63.36%, 33.42%, 1.95%, and 1.27% respectively in increasing order of severity. This is in contrast with the observations made by Narula *et al.* (2017), in which most of the mainland of India was reported to observe moderate exposure condition. The present analysis using the most recent 30 years of data observes a shift in the severity level to the shielded conditions. This is indicative of the receding pattern of driving rain loads for the subcontinent.

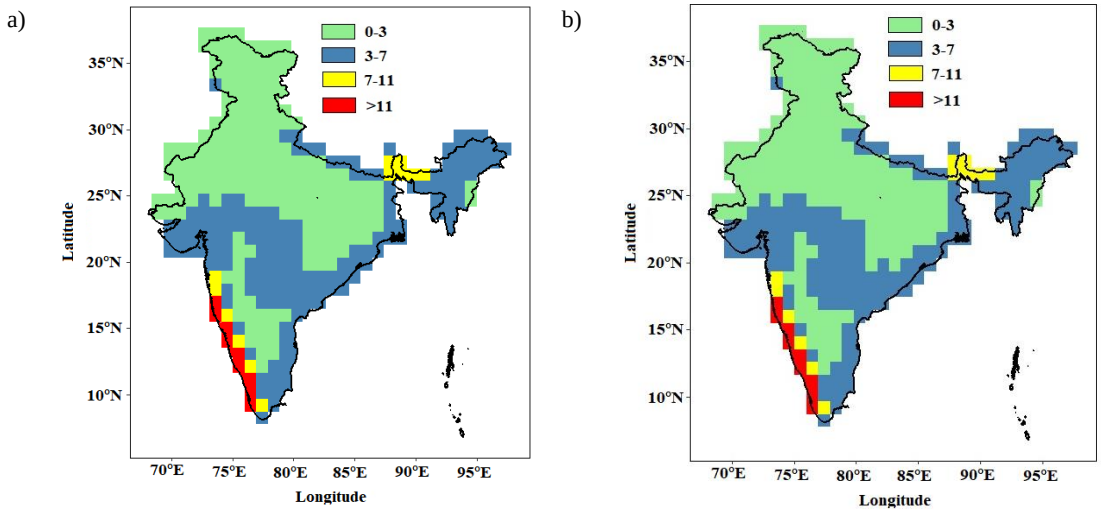

Figure 2. Driving rain map of India based on *maDRI* (a) including and (b) excluding months with no rainfall.

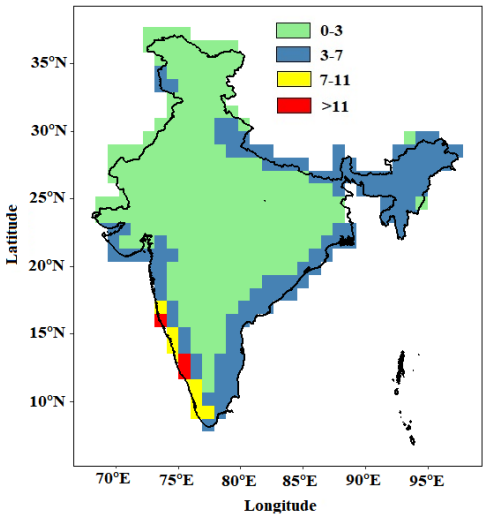

Figure 3. Driving rain map of India based on *aaDRI*.

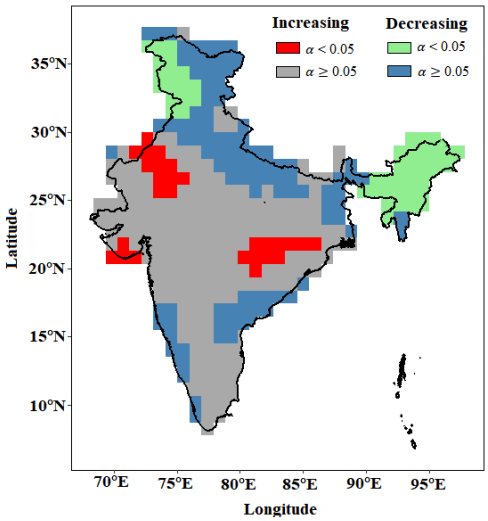

Figure 4. Trend analysis of WDR based on *yDRI*.

Fig. 3 shows the *aaDRI* map of India. Comparison of the *aaDRI* map with *maDRI* map shows a significant increase in the number of grids observing shielded exposure conditions. The percentage of area covered by each exposure category based on *aaDRI* is 77.01%, 21.37%, 1.36%, and 0.25%, respectively, in increasing order of severity. The observation suggests that implementation of *aaDRI* underestimates the driving rain severity at a given location. Therefore, *maDRI* is a more reliable choice for contemplating driving rain severity. For instances when meteorological records are not available at a finer temporal scale, the *aaDRI* can be used towards estimation of *maDRI*. In the following section, a relationship between *maDRI* and *aaDRI* has been established to facilitate the objective.

4.2 Relationship Between *maDRI* and *aaDRI*

The scatter plot between *maDRI* and *aaDRI* values presented in Fig. 5 indicates a fairly strong linear relationship between the two indices. This was also reported in previous studies for India. The relationship obtained between the two indices is given in Eq. 7 and those reported by Chand and Bhargava (2002) and Narula *et al.* (2017) are stated in Eqs. 8 and 9, respectively:

$$maDRI = 1.29 aaDRI - 0.28 \tag{7}$$

$$maDRI = 1.24 aaDRI - 0.18 \tag{8}$$

$$maDRI = 1.23 aaDRI - 0.32 \tag{9}$$

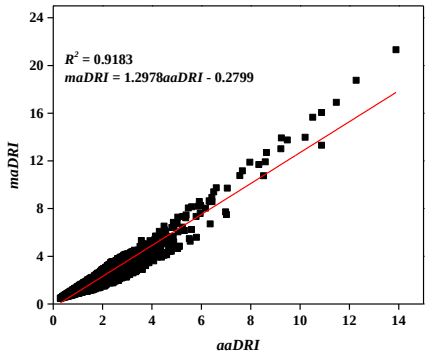

Figure 5. Relationship between *maDRI* and *aaDRI*.

A fair degree of match is observed between the expression reported in this study and those from the previous studies. This indicates the reliability of the indices determined using 0.5°×0.5° gridded data in the present study. The relationship would also aid towards the estimation of *maDRI* from *aaDRI* in instances wherein meteorological records of wind and rainfall are not available at a fine temporal resolution.

4.3 Trend Analysis Based on Yearly Driving Rain Index

This study extends to the determination of any existing trend between the driving rain index for the considered 30 years of data. This is facilitated by determination of yearly driving rain index (*yDRI)* for each year, calculated as stated in Eq. 10:

$$yDRI = (Total\ rainfall\ in\ a\ year) \times \left(Average\ rainfall\ in\ a\ year \right) \quad (10)$$

Rainfall in expressed in *m*, and the average wind speed is expressed in *m/s*. The objective is facilitated by conducting MK test and determination of Sen's slope for each of the grid as discussed in section 3.2. Fig. 4 shows the plot of trend analysis for each of the 1179 grids at 5% significance (α). It can be observed from Fig. 4 that, there exists significant negative trend in northern and north-eastern part of the country, where as significant positive trend is observed by parts of western and south-western India which observe shielded exposure condition. The value of β ranged between [-0.10, 0.04] which is fairly similar to the range of [-0.12, 0.03] as was reported by Narula *et al*. (2017). Out of the total number of grids exhibiting significant trend, 61.53% observe a negative trend in severity.

5 Summary and Conclusion

The present study assesses the severity of prevailing moisture loads on buildings in India at a spatial resolution of 0.5° × 0.5° using gridded records of wind and rainfall data. This assessment has been facilitated by the computation of *maDRI* and *aaDRI*. Trend analysis of yearly driving rain index has also been carried out at a 5% significance level to determine the temporal evolution of the relative severity of moisture loads. The major findings and contributions of this study are as follows:

- *aaDRI* and *maDRI* maps for India at 0.5°×0.5° spatial resolution have been developed.
- The *maDRI* map developed is apt for the assessment of relative severity of moisture loads for India. Zones of shielded, moderate, high, and severe exposure condition correspond to 63.36%, 33.42%, 1.95%, and 1.27% respectively of the total land area.
- There has been a decline in moisture loads manifesting on buildings. Majority of the area has been observed to be under shielded exposure condition, in comparison to a previous study wherein maximum area was reported to be under moderate exposure condition.
- *maDRI* and *aaDRI* exhibit strong linear relationship which is in compliance with previous studies, thus indicating the reliability of the equation developed (Eq. 7) for the determination of *maDRI*.
- Trend analysis of the *yDRI* values reveals statistically significant decreasing trends over the northern and eastern regions of the country whereas increasing trends in the shielded regions surrounding central India.
- The limitation of the reported results lies in the unavailability of fine resolution gridded wind data from ground observations and the lack of grid-to-point comparison of gridded datasets with respect to station data in order to assess the reliability of the gridded weather datasets.

The study can be further be extended towards the determination of daily driving rain index for the same spatial resolution subjected to the availability of data. This is expected to provide a better representation of the prevailing moisture loads on building envelopes in India.

Acknowledgements

The authors acknowledge the ECR grant (No. ECR/2016/001240) provided by SERB, DST for the project "Modelling of hydraulic diffusivity and its application in FE-simulation of moisture transport in concrete for assessing corrosion risk."

ORCID

Sneha Das: https://orcid.org/0000-0003-2262-671X
Kaustav Sarkar: https://orcid.org/0000-0002-8541-1866

References

Bhattacharjee, B. (2013). Moisture influence on the thermal properties of materials in building envelopes and sustainability in tropical climates. In *ICSDEC 2012: Developing the Frontier of Sustainable Design, Engineering, and Construction*, 765-774.

Blocken, B., Abuku, M., Roels, S. and Carmeliet, J. (2009). Wind-driven rain on building facades: some perspectives. *EACWE*, *5*, 19-23.

Bornehag, C.G., Blomquist, G., Gyntelberg, F., Järvholm, B., Malmberg, P., Nordvall L, Nielsen, A., Pershagen G. and Sundell. J. (2001). Dampness in buildings and health. review. Nordic Interdisciplinary review of the Scientific Evidence on Associations between Exposure to Dampness in Buildings and Health Effects (NOrDDAMP). *Indoor Air*, *11*, 72-86.

Broomfield, J.P. (2006). Corrosion of steel in concrete: understanding, investigation and repair. *CRC Press*.

Chand, I. and Bhargava, P.K. (2002). Estimation of driving rain index for India. *Building and Environment*, *37*(5), 549-554.

Charola, A.E. (2000). Salts in the deterioration of porous materials: an overview. *Journal of the American institute for conservation*, *39*(3), 327-343.

Das, S., Narula, P. and Sarkar, K. (2020). Design of intermittent rainfall-pattern for structures with gridded data: Validation and implementation. *Journal of Building Engineering*, *27*, 100939.

Gaylarde, C., Silva, M.R. and Warscheid, T. (2003). Microbial impact on building materials: an overview. *Materials and Structures*, *36*(5), 342-352.

Giarma, C. and Aravantinos, D. (2011). Estimation of building components' exposure to moisture in Greece based on wind, rainfall and other climatic data. *Journal of Wind Engineering and Industrial Aerodynamics*, *99*(2-3), 91-102.

Harris, I.P.D.J., Jones, P.D., Osborn, T.J. and Lister, D.H. (2014). Updated high- resolution grids of monthly climatic observations–the CRU TS3. 10 Dataset. *International journal of climatology*, *34*(3), 623-642.

Hoppestad, S. (1955). Slagregn i Norge (Driving rain in Norway). *NBI Rep*, *13*.

Jerman, M. and Černý, R. (2012). Effect of moisture content on heat and moisture transport and storage properties of thermal insulation materials. *Energy and Buildings*, *53*, 39-46.

Lacy, R.E. (1965). Driving rain maps and the onslaught of rain on buildings. In *Proc. of CIB/RILEM Symposium on Moisture Problems in Buildings, Helsinki, 1965*.

Lacy, R.E. (1977). Climate and building in Britain.

Mann, H.B. (1945). Non-parametric tests against trend. Econometria. *1945. 246*.

Narula, P., Sarkar, K. and Azad, S. (2017). Driving rain indices for India at 1°× 1° gridded scale. *Journal of Wind Engineering and Industrial Aerodynamics*, *161*, 1-8.

National Oceanic and Atmospheric Administration (NOAA), (2019). (http://www/esrl.noaa.gov/psd/data/gridded/data.ncep.reanalysis.derived.surface.html).

Neville, A. (1995). Chloride attack of reinforced concrete: an overview. *Materials and Structures*, *28(2)*, 63.

Pérez-Bella, J.M., Domínguez-Hernández, J., Rodríguez-Soria, B., del Coz-Díaz, J.J. and Cano-Suñén, E. (2012). Estimation of the exposure of buildings to driving rain in Spain from daily wind and rain data. *Building and Environment*, *57*, 259-270.